

# Multi-Gyr History of Mars' CO<sub>2</sub>-Dominated Atmosphere: New Data and a New Synthesis

A.O. Warren (1), **E.S. Kite (2)**, J.-P. Williams (2), B. Horgan (3). (1) University of Chicago, (aowarren@uchicago.edu), (2) UCLA, (3) Purdue University.

**1. Introduction.** Changes in Martian atmospheric pressure over time are an important control on Mars' climate evolution. Most constraints for Martian atmospheric pressure over time are indirect. A direct method uses minimum crater size to estimate an upper limit on atmospheric pressure [1,2]. Thin planetary atmospheres allow small objects to reach the surface at high velocities, forming hypervelocity impact craters [3]. This method is useful for constraining atmospheric pressure during deposition/alteration of ancient sedimentary rocks on Mars with evidence for surface liquid water, as demonstrated by [2] for channel deposits in Aeolis Dorsa. However, finding paleopressure estimates for sites of multiple ages gives us better temporal coverage of paleopressure evolution. Here we report paleopressure data for 2 new sites. are  $<(1.9 \pm 0.1)$  bar at/before 4 Ga (Mawrth paleosurf), and  $<(1.5 \pm 0.1)$  bar at  $\sim 3.8$  Ga (Mawrth Phyllosilicates and Meridiani) (Fig. 1).

**2. Integrating New Paleopressure Results.** The Mawrth phyllosilicates are the oldest known hydrosilyly altered sedimentary rocks in the Solar System (4.3-3.8 Ga [4]), and suggest surface temperatures  $>273\text{K}$  [5]. The phyllosilicates overlie an even more ancient ( $>4$  Gyr) paleosurface [4] with a high density of preserved exhumed ancient craters. This paleosurface may record a signal of changing impactor population over time. Our Meridiani Planum site ( $\sim 3.8$  Ga [7]) features sedimentary units indicative of the presence of surface liquid water during their deposition (e.g. [8]). We use HiRISE orthoimages, anaglyphs, and digital terrain models (DTMs) to identify exhumed ancient craters at our 2 sites and compare the size-frequency distribution of measured crater populations to predictions from an atmosphere-impactor interaction model [9] for atmospheres of different pressures [2]. Assuming pressure to be constant over the duration of crater population accumulation, our new paleopressure limits

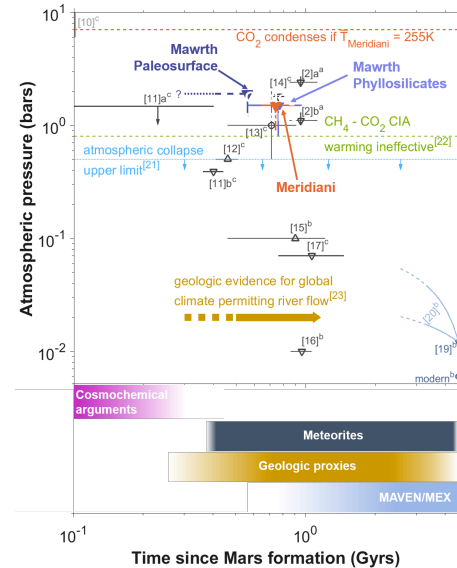
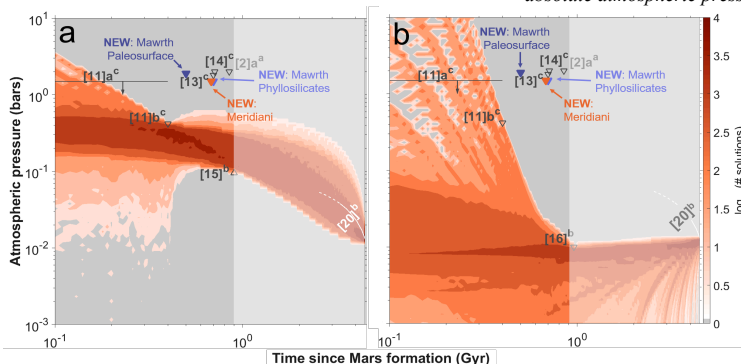


Fig 1 - Updated paleopressure constraints for Mars. Numbers correspond to reference list. Superscripts: *a* - constraints from exhumed ancient craters, *b* remote sensing, *c* - all other methods. [17]c (since superceded by experimental results, see [18]), modern *b* - annual mean modern atmospheric pressure. Modern MAVEN O loss rates [20]b (assumed all due to CO<sub>2</sub>) extrapolated backwards in time. Colored bars - approximate temporal extent of methods for constraining paleopressure. Upward/downward facing triangles indicate lower/upper bounds. Circles - estimates of absolute atmospheric pressure/direct measurements.

Fig 2- Paleopressure histories allowed by existing data. Solution density plots of pressure histories for 10,000 combinations of  $k_1-k_4$ . Grey areas do not match data.  $\log_{10}(\# \text{ solutions}) = \text{all}$  solutions pass through point. a) lowest constraint at  $\sim 3.8$  Ga is  $6^\circ$  b)  $8^\circ$ . Constraints as for Fig 1. Washed out region - no paleopressure estimates exist 3.6 Ga - present, solutions not well constrained.

**3. Bridging direct measurements, meteorites and modelling:** Detailed Mars atmospheric evolution models rely on balancing fluxes from processes such as impact delivery/erosion, outgassing, and loss to space, for which many assumptions are necessary. We used a basic 2-component model starting at present day annual mean atmospheric pressure (including CO<sub>2</sub> in ice caps as estimated from SHARAD data [19]<sup>b</sup>) and measured MAVEN/MEX O loss rates [20]<sup>b</sup>. Our paleopressure upper limits are 2 points among many others that come from meteorite isotope data [11,12], rover sedimentology [15,16], and modelling results [11,12,13,14,17]. To integrate our results with existing knowledge, we built a basic, 2-component, process-agnostic model for Mars' paleopressure evolution constrained by existing data. We gather sources and sinks into 1 term, expressed as either a powerlaw ( $\Delta P_{\text{source/sink}} = k_1 t^{1/3} (-k_2/4)$ ) or an exponential ( $\Delta P_{\text{source/sink}} = k_1 t^{1/3} \exp(-t/k_2/4)$ ) with free parameters  $k_1$ ,  $k_2$  (sinks),  $k_3$  &  $k_4$  (sources). Parameters  $\{k_1, k_2, \dots, k_4\}$  are found using upper limits of existing paleopressure estimates (excluding [12]<sup>a</sup>, [13]<sup>c</sup> & [2]<sup>b</sup> – Fig 1) as hard constraints on permitted pressure histories. Our model is sensitive to the lowest implemented pressure constraint ([15]<sup>b</sup> or [16]<sup>b</sup>; Fig 2). However, most solutions cluster around initial atmospheric pressures <1 bar irrespective of the minimum paleopressure constraint. This is consistent with upper limits on atmospheric pressure from atmospheric evolution models based on ALH84001 isotope data ([11]<sup>a</sup>).

**4. Climate implications from ~4–3.8 Ga:** It is possible for atmospheric pressure to vary on both short and long timescales through atmospheric collapse through condensation into CO<sub>2</sub> ice sheets at pressures <0.5 bar (e.g [21]) and 100 Myr-timescale processes such as outgassing, impact erosion/delivery of volatiles, atmospheric escape to space, and carbonate formation [24]. Additionally, small craters are preferentially obliterated by sedimentation due to their reduced topographic expression, are less likely to be exposed by erosional cuts through a cratered volume [25], and are more likely to be missed in crater counts due to insufficient DTM/anaglyph resolution. It is possible to reproduce our measured CSFDs by modifying CSFDs for time-varying atmospheric pressure to preferentially remove small craters, provided that the minimum atmospheric pressure is less than our upper limits. To reproduce the number of 15.6–22.1m diameter craters at our Meridiani site, a minimum of 50kyrs must be spent at pressures <<0.1 bar. Therefore, our results suggest 3 end-member paleopressure histories from ~4–3.8 Ga (Fig 3). (1) Maximum pressure <0.5 bar with episodes of condensation of CO<sub>2</sub> into ice caps, (2) pressure

persistently below our upper limits, (3) pressure changes of several bar due to changes in atmospheric sources/sinks.

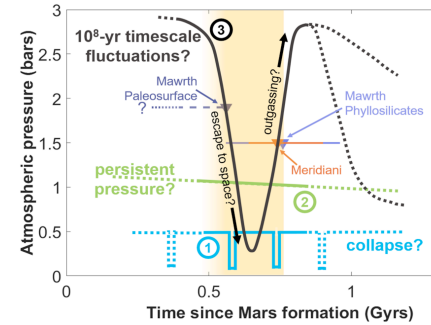


Fig 3 – Schematic illustration of 3 possible end-member cases for Mars' atmospheric pressure history for ~4–3.8 Ga (yellow area). Dotted lines: pressure not directly constrained.

More paleopressure estimates are needed. For example, there are few paleopressure constraints 3.6 to <<1 Ga (Fig 1). More precise chronologies for climate-altering events such as the end of the Martian dynamo and the growth of Tharsis, would constrain the feasibility of scenario #3. Additionally, improved absolute dating of sedimentary deposits would reduce the uncertainty on the ages of our sites and better constrain the intervals in which Mars had rivers.

**Acknowledgements:** J. Sneed (HiRISE DTMs; pipeline: [25]). Grants: NASA (NNX16AJ38G).

**References.** [1] Vasavada A. R. et al. (1993) *JGR: Planets*, 98, 3469. [2] Kite E. S. et al. (2014) *Nat. Geosci.*, 7, 335. [3] Tauber M. E. & Kirk D. B. (1976) *Icarus*, 208, 351. [4] Loizeau D. et al. (2012) *P&SS*, 72, 31. [5] Bishop J. et al. (2018) *Nat. Astron.*, 2, 206. [7] Hynek B. M. & Di Achille, G. (2017), *USGS Investigations Map 3356*. [8] Davis J. M. et al. (2016) *Geology*, 44, 847. [9] Williams J.-P. et al. (2014) *Icarus*, 235, 23–36. [10] Lammer H. et al. (2013) *SSR*, 174, 113. [11] Cassata W. S. et al. (2012) *Icarus*, 221, 461. [12] Kurokawa H. et al. (2018) *Icarus*, 299, 443–459. [13] van Berk W. et al. (2012) *JGR Planets*, 117. [14] Hu R. et al. (2015) *Nat. Communications*, 6. [15] Manga M. et al. (2012) *GRL*, 39. [16] Lapôtre M. G. A. et al. 2016 *Science*, 353, 55–58. [17] Bristow T. F. et al. (2017) *PNAS*, 114, 2166–2170. [18] Tosca N. J. et al. (2018) *Nat. Geosci.*, 11, 635. [19] Bierson C. J. et al. (2016) *GRL*, 43, 4172. [20] Lillis R. J. et al. (2015) *SSR*, 195, 357. [21] Forget F. et al. (2013) *Icarus*, 222, 81–99. [22] Turret et al. (2019) *Icarus*, 321, 189. [23] Jakosky B. M. (2018) *Icarus*, 315, 146. [24] Smith M. R. et al. (2008) *GRL*, 35. [25] Mayer D.P. & Kite E.S. (2016) *LPSC XLVII*, abstract #1241.